# Existence and stability of fixed points for a discretised nonlinear reaction–diffusion equation with delay

Desmond J. Higham [*], Tasneem Sardar [1]

*Department of Mathematics and Computer Science, The University of Dundee, Dundee, DD1 4HN, Scotland, UK*

## Abstract

The long-time behaviour of a discretised evolution equation is studied. The equation, which involves diffusion and a nonlinear, delayed, reaction term, has been proposed as a model in population dynamics. It contains, as special cases, logistic-style problems that have been used before to provide canonical examples of *spurious* behaviour. The existence and stability of the basic steady states are systematically studied, as functions of the grid spacings and problem parameters. Particular attention is paid to the effect of the delay on the long-time behaviour. It is found that, as has been seen with other nonlinear problems, increasing the time step beyond the linear stability limit may induce stable, spurious, steady states, which are clearly undesirable as numerical solutions. When a delay is present, spurious solutions are also found to exist within the linear stability limit, and this is seen to affect the dynamics. Potential symmetry in the problem is identified and it is shown that in certain circumstances the bifurcation patterns depend dramatically upon whether the initial data shares the symmetry.

## 1. Introduction

It is now widely recognised that long-time numerical simulations can settle down to unwanted, *spurious*, steady states. Classical convergence and linear stability theory is not relevant in these circumstances and, in general, a bifurcation analysis must be performed for each combination of method and problem. The canonical example of complicated long-time behaviour arising from a discrete map is given by the Euler discretisation of the logistic initial value ordinary differential equation (ODE)

$$u_t = u(t)(1 - u(t)), \quad t > 0, \qquad u(0) = u_0. \tag{1.1}$$

With a stepsize of $\Delta t$, the map is

$$u_{n+1} = u_n + \Delta t u_n (1 - u_n), \quad n \geqslant 0. \tag{1.2}$$

The resulting bifurcation diagram for this map can be found in many texts; see, for example, [15,17,18]. In fact, the difference in emphasis between these three references illustrates that the same map can be analysed in a number of contexts:

- in an application where the map itself is a mathematical model,
- in the theoretical study of dynamical systems,
- in the analysis of numerical methods, where the map is regarded as an approximation to an underlying continuous problem.

In particular, we point out that a numerical analyst may regard a long-term solution as *spurious* while, in a different context, the solution may be interpreted as *interesting* by a mathematical biologist. From a numerical analysis perspective, it is essential that the asymptotic, $n \to \infty$, behaviour of the map reflects the dynamics of the continuous problem. Studying simple, nonlinear problems, such as (1.1) gives insight into the difficulties that may arise.

There are many ways in which to alter, or generalise, the problem (1.1) and the numerical method used to give (1.2). Griffiths et al. [7] consider explicit Runge–Kutta methods on polynomial-type ODEs. Griffiths and Mitchell [6] and Gardiner and Mitchell [4] add diffusion in (1.1) to give an initial-boundary value partial differential equation (PDE) with periodic and homogeneous Dirichlet boundary values, respectively. This reaction–diffusion equation, which is often referred to as Fisher's equation, is a standard model in population dynamics [15]. Discrete and semi-discrete analogues of the PDE have also been proposed as biological models [13]. It is often argued that, as a population model, the logistic ODE can be made more realistic by including delay effects. A finite difference approximation to an ordinary delay differential equation (DDE) analogue of (1.1) was studied in [9].

In this work we perform a systematic study of the basic steady states that are possible when both diffusion and a constant delay are incorporated in (1.1). The continuous model, which is known as Hutchinson's equation [3], is discretised with central differences in space and Euler's method in time. To allow for the delay, we use a linear Lagrange interpolant, which is a natural continuous extension of the Euler step. We impose homogeneous Dirichlet boundary values— this is perhaps the most relevant choice for applications in population dynamics. Our approach is ODE-based: we first discretise in space with the method of lines, and then consider the time discretisation. We emphasise that the semi-discrete problem itself may be regarded as the underlying model in some circumstances—for example, in *island chains*, where individuals inhabit separate regions, with some interaction between neighbouring regions [5]. Hence, even a very coarse space discretisation (which, in this work, turns out to give the most tractable problem) may be of interest.

Our aim, as numerical analysts, is to understand how the existence and stability of the steady states vary with the grid parameters. The analysis is specialised to one problem and discretisation. However, we feel that the problem is sufficiently general to make the results of interest. In addition to the widely-recognised feature of spurious solutions bifurcating beyond the linear stability limit, we look at the following issues:

- the dependence on the diffusion and delay coefficients of the existence and stability of fixed points,

- the effect of symmetry on the bifurcation patterns (even in the presence of rounding errors),
- the potential for spurious solutions within the linear stability limit when a nonzero delay is present.

Section 2 defines the continuous problem, sets up the discretisation and looks at the semi-discrete problem. In Section 3, we consider the zero-delay case. Here we extend some results from [4]. In particular, we show how different bifurcation patterns can arise depending on the symmetry in the problem. Section 4 covers the general case of a non-zero delay. In the final section we present our conclusions and point out areas for future work.

Our policy in this paper is to focus on the presentation and interpretation of the main results. Further technical details can be found in the report [11].

## 2. Hutchinson's equation (HE)

### 2.1. Hutchinson's equation and space discretisation

Consider Hutchinson's equation

$$\frac{\partial}{\partial t} u(x, t) = \varepsilon \frac{\partial^2}{\partial x^2} u(x, t) + u(x, t)[1 - u(x, t - \tau)], \qquad t > 0, \quad x \in (0, 1); \qquad (2.1)$$

$$u(x, t) = \Psi(x, t), \qquad t \in [-\tau, 0], \quad x \in (0, 1),$$

subject to homogeneous Dirichlet boundary conditions:

$$u(0, t) = u(1, t) = 0, \quad t \geqslant -\tau,$$

where $\varepsilon > 0$ is the diffusion coefficient, $\tau > 0$ is the amount of delay and the "initial value function" $\Psi(x, t)$ is continuous. For the purpose of comparison, we also consider the non-delay version, for which $\tau = 0$.

The scalar partial DDE (2.1) is initially transformed into a system of ordinary delay differential equations by discretising the space variable $x$ into $(N + 1)$ discrete values $(N \geqslant 2)$, with a constant stepsize in space, $\Delta x = 1/N$, so that $x_j = j \Delta x$, $j = 0, 1, \ldots, N$. Let $\Phi_j(t) = \Psi(x_j, t)$ and $U_j(t)$ denote the approximation to $u(x_j, t)$. Using the standard central difference operator to approximate the Laplacian we obtain the system

$$\frac{d}{dt} U(t) = \frac{\varepsilon}{\Delta x^2} M U(t) + U(t) \circ [e - U(t - \tau)], \quad t > 0; \qquad (2.2)$$

$$U(t) = \Phi(t), \quad t \in [-\tau, 0],$$

where $U(t - \tau), U(t), \Phi(t) \in \mathbb{R}^{N-1}$, $e = [1, 1, \ldots, 1]^T \in \mathbb{R}^{N-1}$ and

$$M = \begin{bmatrix} -2 & 1 & & & & \\ 1 & -2 & \ddots & & & \\ & \ddots & \ddots & \ddots & & \\ & & \ddots & \ddots & 1 \\ & & & 1 & -2 \end{bmatrix} \in \mathbb{R}^{(N-1)\times(N-1)}.$$

The symbol " $\circ$ " denotes componentwise multiplication, so that

$$
\begin{bmatrix} u_1 \\ \vdots \\ u_{N-1} \end{bmatrix} \circ \begin{bmatrix} w_1 \\ \vdots \\ w_{N-1} \end{bmatrix} := \begin{bmatrix} u_1 w_1 \\ \vdots \\ u_{N-1} w_{N-1} \end{bmatrix}.
$$

## 2.2. Fully discretised Hutchinson's equation

To solve the system of DDEs (2.2), Euler's method is applied to advance the solution in time and a linear Lagrange interpolant, $q(t - \tau)$, is used to approximate the delayed values, $U(t - \tau)$.

Setting $t_n = n\Delta t$, where $\Delta t$ is a positive constant stepsize in time, let $U^n$ denote the approximation to $U(t_n)$. Euler's method applied to (2.2) gives

$$
U^{n+1} = U^n + r_\varepsilon M U^n + \Delta t U^n \circ [e - q(t_n - \tau)], \quad n \geqslant 0, \tag{2.3}
$$

where $q(t_n - \tau) \simeq U(t_n - \tau)$ and

$$
r_\varepsilon = \varepsilon \frac{\Delta t}{\Delta x^2} = \varepsilon N^2 \Delta t.
$$

If $t_n - \tau \leqslant 0$, then we can take $q(t_n - \tau) = \Phi(t_n - \tau)$. Otherwise, let $m$ be the smallest integer such that $\tau \leqslant m\Delta t$. Then $t_n - \tau$ lies in the interval $[t_{n-m}, t_{n-m+1})$; that is, $(m-1)\Delta t < \tau \leqslant m\Delta t$. Let $\sigma\Delta t = m\Delta t - \tau$, so that

$$
\sigma = m - \frac{\tau}{\Delta t}, \quad \sigma \in [0, 1).
$$

The linear Lagrange interpolant based on the values $U^{n-m+1}$ and $U^{n-m}$ is then given by

$$
q(t_n - \tau) = \sigma U^{n-m+1} + (1 - \sigma)U^{n-m}.
$$

Hence, on a general step with $t_n > \tau$ we have the recurrence

$$
U^{n+1} = U^n + r_\varepsilon M U^n + \Delta t U^n \circ [e - \sigma U^{n-m+1} - (1 - \sigma)U^{n-m}], \quad n \geqslant 0. \tag{2.4}
$$

Let

$$
v^n := \begin{bmatrix} U^n \\ U^{n-1} \\ \vdots \\ U^{n-m} \end{bmatrix} \in \mathbb{R}^{(N-1)(m+1)}
$$

and define $f(v^n) \in \mathbb{R}^{N-1}$ by

$$
f(v^n) := (1 + \Delta t)U^n + r_\varepsilon M U^n - (m\Delta t - \tau)[U^n \circ U^{n-m+1}]
$$

$$
+ (m\Delta t - \tau - \Delta t)[U^n \circ U^{n-m}]. \tag{2.5}
$$

Table 1
Period-(1, 1) solutions and their linear stability

| $N$ | Constant solution $U^*e$ | Linearly stable | |
|-----|--------------------------|-----------------|---|
| $N \geqslant 2$ | $U^* = 0$ | $\varepsilon > \varepsilon_N$ | $\tau \geqslant 0$ |
| $N = 2$ | $U^* = 1 - 8\varepsilon$ | $\varepsilon < \dfrac{1}{8}$ | $0 \leqslant \tau < \dfrac{\pi}{2(1-8\varepsilon)}$ |
| $N = 3$ | $U^* = 1 - 9\varepsilon$ | $\varepsilon < \dfrac{1}{9}$ | $0 \leqslant \tau < \dfrac{\pi}{2(1-9\varepsilon)}$ |
| $N \geqslant 4$ | no nonzero $U^*$ | | |

Then (2.4) may be written in the form $v^{(n+1)} = G(v^n)$, where

$$\begin{bmatrix} U^{n+1} \\ U^n \\ \vdots \\ U^{n-m+1} \end{bmatrix} = G\left( \begin{bmatrix} U^n \\ U^{n-1} \\ \vdots \\ U^{n-m} \end{bmatrix} \right) := \begin{bmatrix} f(v^n) \\ U^n \\ \vdots \\ U^{n-m+1} \end{bmatrix} \in \mathbb{R}^{(N-1)(m+1)}. \tag{2.6}$$

This is an $(m + 1)$-step vector recurrence, in which the value of $m$ depends upon the stepsize, $\Delta t$.

### 2.3. Constant solutions of partially discretised system

Constant solutions of (2.2) which are period-one in space, that is, of the form $U(t) \equiv U^*e$ with $U^* \in \mathbb{R}$, must satisfy

$$U^*\left[ (\varepsilon N^2)Me + (1 - U^*)e \right] = 0 \in \mathbb{R}^{N-1}.$$

It is easily shown that they exist as given in Table 1.

The linear stability of the zero solution can be determined by examining the appropriate Jacobian matrix. For the nonzero solutions, linear stability theory for DDEs must be applied; see [2]. Table 1 summarises the stability results, including, for comparison, the case $\tau = 0$. The value $\varepsilon_N$ in the table is defined by

$$\varepsilon_N := \frac{1}{2N^2[1 - \cos(\pi/N)]}. \tag{2.7}$$

(This has the asymptotic value $\lim_{N \to \infty} \varepsilon_N = 1/\pi^2$.)

## 3. Dynamics of Hutchinson's equation with zero delay

In order to study the effects of introducing a delay, we first analyse the fixed points of Hutchinson's equation (2.1) with $\tau = 0$. In this case, (2.3) simplifies to $U^{n+1} = g(U^n)$, where

$$g(U^n) = U^n + r_\varepsilon M U^n + \Delta t U^n \circ [e - U^n], \quad n \geqslant 0. \tag{3.1}$$

We note that the Jacobian matrix of this iteration is of the form

$$J(U^n) = (1 + \Delta t)I + r_\varepsilon M - 2\Delta t \; \text{diag}(U^n) \in \mathbb{R}^{(N-1)\times(N-1)}. \tag{3.2}$$

Existence and linear stability of period-(1, 1) and period-(2, 1) solutions for $N = 2$ have been analysed by Gardiner and Mitchell [4]. Their results will be stated here. We will also go into further detail theoretically for larger $N$ and give numerical results where appropriate. Further, we pay attention to the special case of symmetric initial data when $N = 3$.

### 3.1. Period-(1, 1)

The fixed points of (3.1) that are period-one in space and time are solutions satisfying $U^n = g(U^n)$ such that $U^n \equiv U^*e$. These are identical to the ones for (2.2) given in Table 1.
For $N = 3$, we note that the iteration has the form

$$\begin{bmatrix} U_1^{n+1} \\ U_2^{n+1} \end{bmatrix} = \begin{bmatrix} U_1^n \\ U_2^n \end{bmatrix} + r_\varepsilon \begin{bmatrix} -2 & 1 \\ 1 & -2 \end{bmatrix} \begin{bmatrix} U_1^n \\ U_2^n \end{bmatrix} + \Delta t \begin{bmatrix} U_1^n \\ U_2^n \end{bmatrix} \circ \left( \begin{bmatrix} 1 \\ 1 \end{bmatrix} - \begin{bmatrix} U_1^n \\ U_2^n \end{bmatrix} \right). \tag{3.3}$$

It follows that for initial data such that $U_1^0 = U_2^0$, all iterates will satisfy $U_1^n = U_2^n$. Even with finite precision arithmetic, the symmetry in (3.3) ensures that the rounding errors in each component will be the same (under the reasonable assumption that fl($a + b$) = fl($b + a$), where fl is the floating point answer). Hence, the stability of appropriate fixed points when $U_1^0 = U_2^0$ must be treated separately—the action of the Jacobian on $e$ determines the stability. The region of stability when $U_1^0 = U_2^0$ is potentially much larger than that for general initial data.

*Linear stability of zero fixed point*
At the fixed point $U^n \equiv 0$, the Jacobian $J(0) = (1 + \Delta t)I + r_\varepsilon M$ has eigenvalues [14]

$$\lambda_j = (1 + \Delta t - 2r_\varepsilon) + 2r_\varepsilon \cos\left( \frac{j\pi}{N} \right), \quad j = 1, \dots, N - 1,$$

which have modulus less than one for

$$2r_\varepsilon \left[ 1 + \cos\left( \frac{\pi}{N} \right) \right] - 2 < \Delta t < 2r_\varepsilon \left[ 1 - \cos\left( \frac{\pi}{N} \right) \right].$$

Substituting for $r_\varepsilon$, after some manipulation, we find that $U^n \equiv 0$ is linearly stable when $\varepsilon > \varepsilon_N$ and $0 < \Delta t < \Delta t_N$, where

$$\Delta t_N := \frac{2}{2N^2\varepsilon[1 + \cos(\pi/N)] - 1}.$$

We note that, when $N = 3$, $J(0)e = (1 + \Delta t - r_\varepsilon)e$. Hence the condition $|1 + \Delta t - r_\varepsilon| < 1$ determines stability when $U_1^0 = U_2^0$. It follows that when $\varepsilon > \varepsilon_3 = \frac{1}{9}$, the zero solution is linearly stable for $0 < \Delta t < 2/(9\varepsilon - 1)$ if $U_1^0 = U_2^0$, which should be compared with the smaller range $0 < \Delta t < 2/(27\varepsilon - 1)$ that applies for general initial data.

Table 2
Eigenvalues $\lambda_j(J(U^*e))$ at selected values of $\Delta t$

| $N$ | $U^n \equiv U^*e$ | $\varepsilon$ | $\Delta t$ | $\lambda_j(J(U^*e))$ | $\lambda_e$ |
|---|---|---|---|---|---|
| $N = 2$ | $U^* = 0$ | $\varepsilon > \dfrac{1}{8}$ | $\dfrac{2}{8\varepsilon - 1}$ | $-1$ | $-1$ |
| $N = 3$ | $U^* = 0$ | $\varepsilon > \dfrac{1}{9}$ | $\dfrac{2}{27\varepsilon - 1}$ | $-1, \dfrac{9\varepsilon + 1}{27\varepsilon - 1}$ | $\dfrac{9\varepsilon + 1}{27\varepsilon - 1}$ |
| $N = 3$ | $U^* = 0$ | $\varepsilon > \dfrac{1}{9}$ | $\dfrac{2}{9\varepsilon - 1}$ | $-5 - \dfrac{4}{9\varepsilon - 1}, -1$ | $-1$ |
| $N \geqslant 4$ | $U^* = 0$ | $\varepsilon > \varepsilon_N$ | $\Delta t_N$ | $-1, \ldots, -1 + 4N^2\varepsilon \cos(\pi/N)\Delta t_N$ | none |
| $N = 2$ | $U^* = 1 - 8\varepsilon$ | $\varepsilon < \dfrac{1}{8}$ | $\dfrac{2}{1 - 8\varepsilon}$ | $-1$ | $-1$ |
| $N = 3$ | $U^* = 1 - 9\varepsilon$ | $\varepsilon < \dfrac{1}{9}$ | $\dfrac{2}{1 + 9\varepsilon}$ | $-1, \dfrac{27\varepsilon - 1}{9\varepsilon + 1}$ | $\dfrac{27\varepsilon - 1}{9\varepsilon + 1}$ |
| $N = 3$ | $U^* = 1 - 9\varepsilon$ | $\varepsilon < \dfrac{1}{9}$ | $\dfrac{2}{1 - 9\varepsilon}$ | $-\dfrac{27\varepsilon + 1}{1 - 9\varepsilon}, -1$ | $-1$ |
| $N \geqslant 4$ | no nonzero $U^*$ | | | | |

## Linear stability of nonzero fixed points

For $N = 2$, see [4]; the period-one solution $U^n \equiv (1 - 8\varepsilon)e$ is linearly stable for

$$\varepsilon < \frac{1}{8}, \qquad 0 < \Delta t < \frac{2}{1 - 8\varepsilon}.$$

For $N = 3$ the conditions for linear stability are

$$\varepsilon < \frac{1}{9}, \qquad 0 < \Delta t < \frac{2}{1 + 9\varepsilon}.$$

We also note that $J((1 - 9\varepsilon)e)e = (1 - \Delta t + r_\varepsilon)e$, from which it follows that with initial data satisfying $U_1^0 = U_2^0$, the relevant stability condition is

$$\varepsilon < \frac{1}{9}, \qquad 0 < \Delta t < \frac{2}{1 - 9\varepsilon}.$$

Table 2 gives the eigenvalues at the (possible) bifurcation points of $U^n \equiv U^*e$ and, where appropriate, $\lambda_e$ denotes the eigenvalue corresponding to the eigenvector $e$. At the given stepsizes in Table 3.1, a root of the Jacobian passes through $-1$, so period two solutions may bifurcate.

### 3.2. Period-(2, 1)

Fixed points of (3.1) which are period-(2, 1), that is period-one in space and period-two in time, are solutions satisfying $U^n = g(g(U^n)) \neq g(U^n)$ such that $U^n \equiv U_*^n e$, with $U_*^n \in \mathbb{R}$.

For $N = 2$, see [4]; a period-(2, 1) solution with

$$U_*^n = \left[ \frac{(1 - 8\varepsilon)\Delta t + 2}{2\Delta t} + (-1)^n \frac{\sqrt{(1 - 8\varepsilon)^2 \Delta t^2 - 4}}{2\Delta t} \right]$$

exists only for $\Delta t^2 > 4/(1 - 8\varepsilon)^2$, $\varepsilon \neq \frac{1}{8}$. This is linearly stable for

$$\frac{2}{|1 - 8\varepsilon|} < \Delta t < \frac{\sqrt{6}}{|1 - 8\varepsilon|}, \qquad \varepsilon \neq \frac{1}{8}.$$

As expected from Table 2, if $\varepsilon > \frac{1}{8}$, then this period bifurcates from the stepsize $\Delta t = 2/(8\varepsilon - 1)$ at which the period-(1, 1) solution $U^n \equiv 0$ becomes unstable, and if $\varepsilon < \frac{1}{8}$ then this period bifurcates from the stepsize $\Delta t = 2/(1 - 8\varepsilon)$ at which the period-(1, 1) solution $U^n \equiv (1 - 8\varepsilon)e$ becomes unstable.

For $N = 3$, a period-(2, 1) solution with

$$U_*^n = \left[ \frac{(1 - 9\varepsilon)\Delta t + 2}{2\Delta t} + (-1)^n \frac{\sqrt{(1 - 9\varepsilon)^2 \Delta t^2 - 4}}{2\Delta t} \right],$$

is found to exist for $\Delta t^2 > 4/(1 - 9\varepsilon)^2$, $\varepsilon \neq \frac{1}{9}$. With general initial data, this solution is linearly stable when $\varepsilon < \frac{1}{27}$ and

$$\frac{2}{(1 + 9\varepsilon)(1 - 27\varepsilon)} \left[ 9\varepsilon + \sqrt{81\varepsilon^2 + (1 + 9\varepsilon)(1 - 27\varepsilon)} \right] < \Delta t < \frac{\sqrt{6}}{1 - 9\varepsilon}. \qquad (3.4)$$

However, when $U_1^0 = U_2^0$ the condition for linear stability is

$$\frac{2}{|1 - 9\varepsilon|} < \Delta t < \frac{\sqrt{6}}{|1 - 9\varepsilon|}, \qquad \varepsilon \neq \frac{1}{9}.$$

With the information for $N = 3$ in Table 2, note that with initial values $U_1^0 \neq U_2^0$ for $\varepsilon < \frac{1}{27}$, this period-(2, 1) solution does not bifurcate from the stepsize $\Delta t = 2/(1 + 9\varepsilon)$ at which the period-(1, 1) solution $U^n \equiv (1 - 9\varepsilon)e$ becomes unstable. However, in the case when the iteration is initiated with $U_1^0 = U_2^0$, if $\varepsilon < \frac{1}{9}$ then this period-(2, 1) solution does bifurcate from the stepsize $\Delta t = 2/(1 - 9\varepsilon)$ at which the period-(1, 1) solution $U^n \equiv (1 - 9\varepsilon)e$ becomes unstable and if $\varepsilon > \frac{1}{9}$ then the solution bifurcates from the stepsize $\Delta t = 2/(9\varepsilon - 1)$ at which the period-(1, 1) solution $U^n \equiv 0$ becomes unstable.

### 3.3. Period-(2, 2)* for $N = 3$

To investigate the bifurcation that occurs when the period-(1, 1) solution becomes unstable for the case when the iteration is initiated with $U_1^0 \neq U_2^0$, we look for fixed points which are period-two in time and space, of the special form

$$U_{**}^{2n} \equiv \begin{bmatrix} a \\ b \end{bmatrix}, \qquad U_{**}^{2n+1} \equiv \begin{bmatrix} b \\ a \end{bmatrix},$$

with $a \neq b$. Following [6] we refer to these as period-(2, 2)* solutions. Note that this form can never arise in the iteration initiated with $U_1^0 = U_2^0$, since in this case $U_1^n = U_2^n$ for all $n$.

For iteration (3.1), the condition $U_{**}^{2n} = g(g(U_{**}^{2n}))$ requires

$$b = a + r_\varepsilon(b - 2a) + \Delta ta(1 - a), \qquad (3.5)$$

$$a = b + r_\varepsilon(a - 2b) + \Delta tb(1 - b), \qquad (3.6)$$

Writing $a$ and $b$ in the form $a = \alpha + \beta$ and $b = \alpha - \beta$, the period-$(2, 2)^*$ solution becomes

$$U_{**}^n = \begin{bmatrix} \alpha + (-1)^n \beta \\ \alpha - (-1)^n \beta \end{bmatrix}. \tag{3.7}$$

When $\Delta t = 1/(9\varepsilon)$ and $\varepsilon \neq \frac{1}{9}$, Eqs. (3.5)–(3.6) give

$$\alpha = \frac{(1 - 9\varepsilon)}{2}, \qquad \beta = \frac{(1 - 9\varepsilon)}{2}. \tag{3.8}$$

It can be shown that solutions of this form are always unstable. When $\Delta t \neq 1/(9\varepsilon)$, (3.5)–(3.6) lead to

$$\alpha = \frac{\left[(1 - 27\varepsilon)\Delta t + 2\right]}{2\Delta t}, \tag{3.9}$$

$$\beta = \frac{\sqrt{\left[(1 - 27\varepsilon)\Delta t + 2\right]\left[(1 + 9\varepsilon)\Delta t - 2\right]}}{2\Delta t}. \tag{3.10}$$

It can be shown that these solutions are linearly stable in the two intervals

$$(2 - r_\varepsilon) < \Delta t < r_\varepsilon + \sqrt{2(3 - 5r_\varepsilon + 2r_\varepsilon^2)}, \tag{3.11}$$

$$r_\varepsilon - \sqrt{2(3 - 5r_\varepsilon + 2r_\varepsilon^2)} < \Delta t < (3r_\varepsilon - 2), \tag{3.12}$$
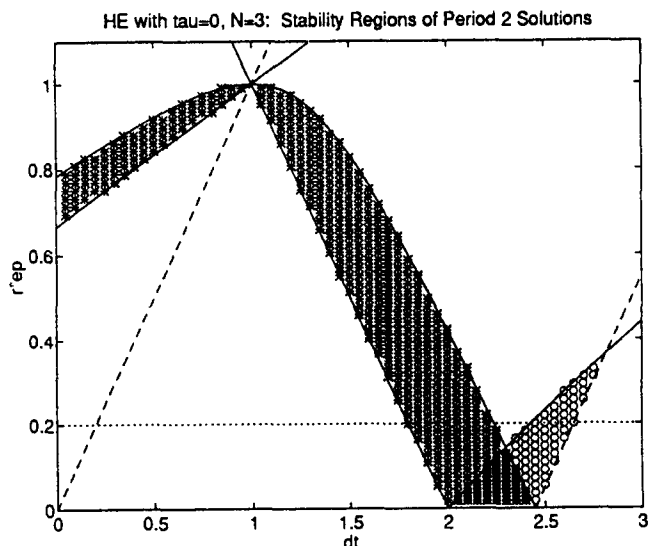


Fig. 1. Linear stability regions when $U_1^0 \neq U_2^0$ in the $\Delta t - r_\varepsilon$ plane.
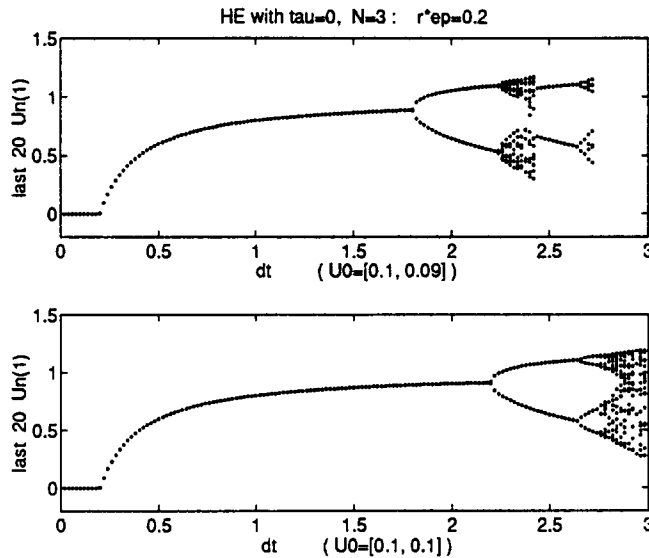
Fig. 2. Long-term behaviour with $r_\varepsilon = 0.2$ for unequal and equal initial data.

where $r_\varepsilon = 9\varepsilon\Delta t$. The corresponding region of the $\Delta t$–$r_\varepsilon$ plane is marked with the " * " symbol in Fig. 1. The stability region of the period-(2, 1) solution when $U_1^0 \neq U_2^0$ is also shown using the symbol " ∘ ".

Note that the region where $U^n \equiv 0$ is stable corresponds to the interior of the triangle with vertices at (0, 0), (1, 1) and $(0, \frac{2}{3})$ in Fig. 1, and for the region where $U^n \equiv (1 - 9\varepsilon)e$ is stable, the vertices are at (0, 0), (1, 1) and (2, 0).

It can be seen from Fig. 1, or by manipulating (3.11)–(3.12), that for $\varepsilon < \frac{1}{9}$, a stable period-(2, 2)* solution bifurcates from the stepsize $\Delta t = 2/(1 + 9\varepsilon)$ at which the period-(1, 1) solution $U^n \equiv (1 - 9\varepsilon)e$ becomes unstable and for $\varepsilon > \frac{1}{9}$, a stable period-(2, 2)* solution bifurcates from the stepsize $\Delta t = 2/(27\varepsilon - 1)$ at which the period-(1, 1) solution $U^n \equiv 0$ becomes unstable.

A bifurcation diagram for the case $r_\varepsilon = 0.2$ (that is, $\varepsilon = 0.2/(9\Delta t)$) is given in Fig. 2. Here the time step ranges from 0 to 3 on the $x$-axis. For each time step we performed 1000 iterations, plotting the first component of the last 20 iterates. The top picture comes from unequal initial data, $U^0 = [0.1, 0.09]^T$, and the lower picture has equal initial data, $U^0 = [0.1, 0.1]^T$. Note that $\varepsilon > \frac{1}{9}$ when $\Delta t < 0.2$ and $\varepsilon < \frac{1}{9}$ when $\Delta t > 0.2$. As expected, the zero fixed point is stable in the range $0 < \Delta t < 0.2$ for both types of initial condition. With $U_1^0 \neq U_2^0$ (in the top diagram) the nonzero fixed point $U^n \equiv (1 - 0.2/\Delta t)e$ is stable when $0.2 < \Delta t < 1.8$, the special period-(2, 2)* solution (which cannot occur with $U_1^0 = U_2^0$) appears when $1.8 < \Delta t < 2.240$ and the period-(2, 1) solution is only stable when $2.427 < \Delta t < 2.649$. This is highlighted by the horizontal line at $r_\varepsilon = 0.2$ in Fig. 1. On the other hand, with $U_1^0 = U_2^0$ (in the bottom diagram) the nonzero fixed point $U^n \equiv (1 - 0.2/\Delta t)e$ and the period-(2, 1) solution are seen to be stable for the larger ranges $0.2 < \Delta t < 2.2$ and $2.2 < \Delta t < 2.649$, respectively. The difference between taking initial values of the form $U_1^0 \neq U_2^0$ and $U_1^0 = U_2^0$ can be clearly seen in the range $1.8 < \Delta t < 2.427$.

Table 3
Summary of stability of fixed points for $\tau = 0$ with $U_1^0 \neq U_2^0$

| $\varepsilon$ | Period | Form of $U^n$ | Linear stability region with $U_1^0 \neq U_2^0$ |
|---|---|---|---|
| $\varepsilon < 1/27$ | (2, 1) | $U_*^n e$ | $r_\varepsilon + 2\omega_1(r_\varepsilon) < \Delta t < (r_\varepsilon + \sqrt{6})$ |
| $\varepsilon < 1/9$ | (2, 2)* | $U_{**}^n$ | $(2 - r_\varepsilon) < \Delta t < r_\varepsilon + \omega_2(r_\varepsilon)$ |
| $\varepsilon < 1/9$ | (1, 1) | $(1 - 9\varepsilon)e$ | $r_\varepsilon < \Delta t < (2 - r_\varepsilon)$ |
| $\varepsilon > 1/9$ | (1, 1) | $0e$ | $(3r_\varepsilon - 2) < \Delta t < r_\varepsilon$ |
| $\varepsilon > 1/9$ | (2, 2)* | $U_{**}^n$ | $r_\varepsilon - \omega_2(r_\varepsilon) < \Delta t < (3r_\varepsilon - 2)$ |

Table 4
Summary of stability of fixed points for $\tau = 0$ with $U_1^0 = U_2^0$

| $\varepsilon$ | Period | Form of $U^n$ | Linear stability region with $U_1^0 = U_2^0$ |
|---|---|---|---|
| $\varepsilon < 1/9$ | (2, 1) | $U_*^n e$ | $(2 + r_\varepsilon) < \Delta t < (r_\varepsilon + \sqrt{6})$ |
| $\varepsilon < 1/9$ | (1, 1) | $(1 - 9\varepsilon)e$ | $r_\varepsilon < \Delta t < (2 + r_\varepsilon)$ |
| $\varepsilon > 1/9$ | (1, 1) | $0e$ | $(r_\varepsilon - 2) < \Delta t < r_\varepsilon$ |
| $\varepsilon > 1/9$ | (2, 1) | $U_*^n e$ | $(r_\varepsilon - \sqrt{6}) < \Delta t < (r_\varepsilon - 2)$ |

### 3.4. Summary of linear stability regions for $N = 3$

The results concerning linear stability of fixed points for Hutchinson's equation with $\tau = 0$, when $N = 3$, are summarised in the Tables 3 and 4, where

$$\omega_1(r_\varepsilon) := \sqrt{1 + r_\varepsilon + r_\varepsilon^2}, \qquad \omega_2(r_\varepsilon) := \sqrt{2(3 - 5r_\varepsilon + 2r_\varepsilon^2)}.$$

## 4. Fixed points of fully discretised Hutchinson's equation

### 4.1. Period-(1, 1)

Fixed points of (2.6) that are period-one in space and time are solutions satisfying $U^n \equiv U^* e$ and $U^n = f(v^n)$. These are identical to the ones for (2.2) given in Table 1.

#### 4.1.1. The zero fixed point
It is easily seen that linearising about the zero fixed point removes the effect of the delay. Hence, the stability condition $\varepsilon > \varepsilon_N$ and $\Delta t < \Delta t_N$ that arose for the non-delay case also applies here.

#### 4.1.2. The nonzero fixed point for $N = 2$
When $N = 2$, $f(v^n)$ in the recurrence (2.6) may be written in the form

$$f(v^n) = U^n \left[ 1 + \Delta t(1 - 8\varepsilon) - (m\Delta t - \tau)U^{n-m+1} + (m\Delta t - \tau - \Delta t)U^{n-m} \right].$$

We remark that when $\varepsilon < \frac{1}{8}$ this recurrence is equivalent to the one studied in [9].
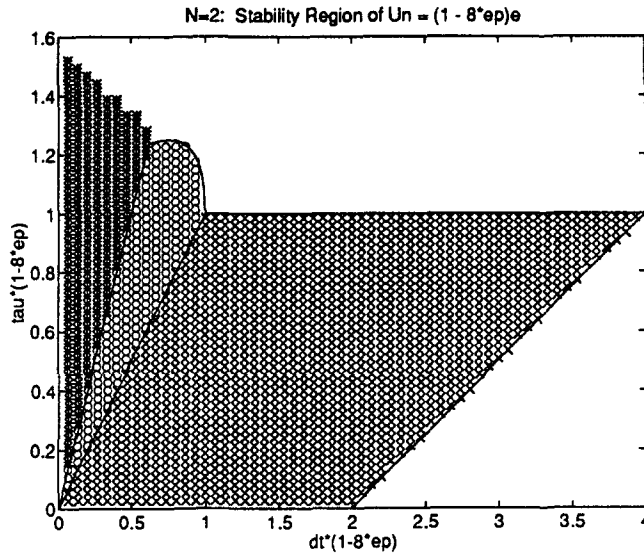
Fig. 3. Region of stability for $U^n \equiv (1 - 8\varepsilon)e$ in the $\Delta t(1 - 8\varepsilon) - \tau(1 - 8\varepsilon)$ plane when $N = 2$. (Also for $U^n \equiv (1 - 9\varepsilon)e$ in the $\Delta t(1 - 9\varepsilon) - \tau(1 - 9\varepsilon)$ plane when $N = 3$ and $\Phi_1(t) = \Phi_2(t)$.)

For $m = 1$, that is, $\Delta t \geqslant \tau$, the region of stability for the fixed point $U^n \equiv (1 - 8\varepsilon)e$ is

$$R_{m=1}^{N=2} := \left\{ \varepsilon, \tau, \Delta t : \varepsilon < \frac{1}{8}, \tau < \frac{1}{(1 - 8\varepsilon)}, \Delta t < 2\left[\tau + \frac{1}{(1 - 8\varepsilon)}\right] \right\}.$$

Similarly, the region for $m = 2$ is

$$R_{m=2}^{N=2} := \left\{ \varepsilon, \tau, \Delta t : \varepsilon < \frac{1}{8}, \Delta t < \frac{1}{(1 - 8\varepsilon)}, \right.$$

$$\left. \Delta t - \frac{\sqrt{1 - \Delta t(1 - 8\varepsilon)}}{(1 - 8\varepsilon)} < \tau < \Delta t + \frac{\sqrt{1 - \Delta t(1 - 8\varepsilon)}}{(1 - 8\varepsilon)} \right\}.$$

The stability region for $m \geqslant 3$ has been determined numerically. It is displayed with the symbol "$*$" in Fig. 3. The linear stability regions for $m = 1$ and $m = 2$ are also shown; they are marked with the symbols "$\times$" and "$\circ$" respectively.

We see from Section 2.3 that for the semi-discrete system, the fixed point is linearly stable for $0 < \tau(1 - 8\varepsilon) < \pi/2$. The region in the figure appears to meet the $y$-axis in the range $(0, \pi/2)$, suggesting that whenever the fixed point is stable for the semi-discrete problem, there exists a time step for which it is stable for the fully discrete problem. This has been verified analytically in [9] and the same technique can be applied to the $N = 3$ case in the next subsection (see Fig. 4).

### 4.1.3. The nonzero fixed point for $N = 3$

When $N = 3$ the iteration has the same symmetry as (3.3). Hence, stability for equal initial data must be treated separately from the general case. It can be shown that when $\Phi_1(t) = \Phi_2(t)$
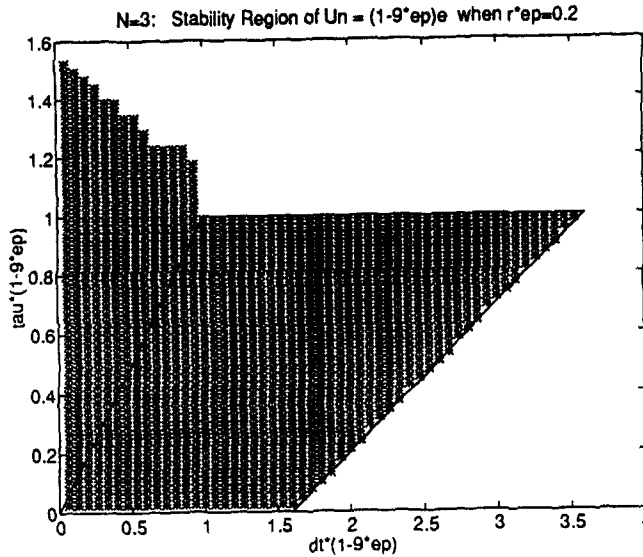
Fig. 4. Region of stability for $U^n \equiv (1 - 9\varepsilon)e$ when $r_\varepsilon = 0.2$ and $\Phi_1(t) \neq \Phi_2(t)$ in the $\Delta t(1 - 9\varepsilon) - \tau(1 - 9\varepsilon)$ plane.

Fig. 3 gives the stability region for $U^n \equiv (1 - 9\varepsilon)e$, if the $x$- and $y$-axes are identified with $\Delta t(1 - 9\varepsilon)$ and $\tau(1 - 9\varepsilon)$, respectively. For $\Phi_1(t) \neq \Phi_2(t)$, when $m = 1$ the region of stability is found to be

$$R_{m=1}^{N=3} = \left\{ \varepsilon, \tau, \Delta t : \varepsilon < \frac{1}{9}, \tau < \frac{1}{(1 - 9\varepsilon)}, \Delta t < \frac{2}{(1 + 9\varepsilon)}[1 + \tau(1 - 9\varepsilon)] \right\},$$

and for $m > 1$ stability occurs when both $p_1(\lambda)$ and $p_2(\lambda)$ are Schur polynomials, where

$$p_1(\lambda) = \lambda^{m+1} - \lambda^m + (m\Delta t - \tau)(1 - 9\varepsilon)\lambda - (m\Delta t - \tau - \Delta t)(1 - 9\varepsilon),$$

$$p_2(\lambda) = \lambda^{m+1} - (1 - 2r_\varepsilon)\lambda^m + (m\Delta t - \tau)(1 - 9\varepsilon)\lambda - (m\Delta t - \tau - \Delta t)(1 - 9\varepsilon).$$

Note that as $r_\varepsilon \to 0$, the polynomial $p_2(\lambda)$ tends to the polynomial $p_1(\lambda)$. We also mention that when $\Phi_1(t) = \Phi_2(t)$ stability is determined by the characteristic equation $p_1(\lambda) = 0$. This emphasises that equal initial data gives rise to a smaller class of perturbations, so that linear stability is a less stringent requirement.

Fig. 4 is an example of a linear stability region, displayed with the symbol " $*$ ", when $r_\varepsilon$ is kept constant; $r_\varepsilon = 0.2$ in this case. The region is plotted in the $\Delta t(1 - 9\varepsilon) - \tau(1 - 9\varepsilon)$ plane, which allows comparison with Fig. 3 for the case when $\Phi_1(t) = \Phi_2(t)$.

The numerically determined linear stability region of $U^n \equiv (1 - 9\varepsilon)e$, that is, the region where $p_1(\lambda)p_2(\lambda) = 0$ is Schur, is given in Fig. 5 for some selected values of $\tau$. The regions are plotted in the $\Delta t - r_\varepsilon$ plane. Note that, from Section 3.4, when $\tau = 0$ the stability region is the interior of the triangle with vertices at $(0, 0)$, $(1, 1)$ and $(2, 0)$. It can be seen that introducing a small delay improves the stability of the iteration.
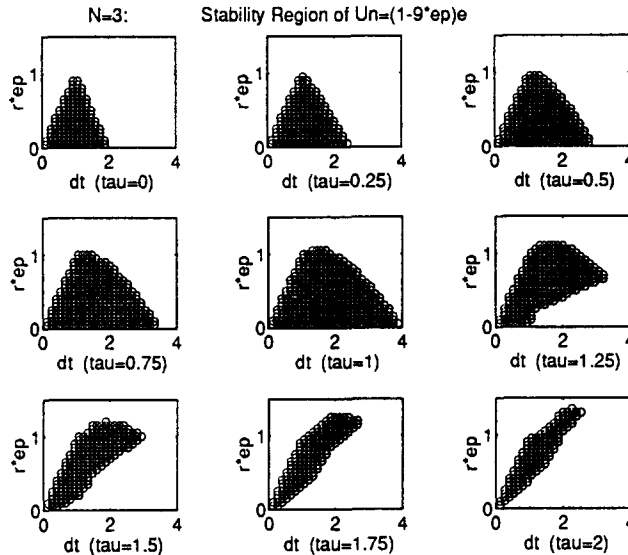
Fig. 5. Regions of stability for $U^n \equiv (1 - 9\varepsilon)e$ when $\Phi_1(t) \neq \Phi_2(t)$, for various $\tau$, in the $\Delta t - r_\varepsilon$ plane.

## 4.2. Period-(2, 1)

Fixed points of (2.6) that are period-(2, 1) are solutions satisfying $U^n \equiv U_*^n e$ and $v_*^n = G(G(v_*^n)) \neq G(v_*^n)$. Let

$$\eta_\varepsilon := \begin{cases} 1 - 8\varepsilon, & \text{if } N = 2, \\ 1 - 9\varepsilon, & \text{if } N = 3, \end{cases}$$

then the period-(2, 1) solution, for both $N = 2$ and $N = 3$, takes the following form.

If $m$ is odd, $\Delta t \neq \tau/m$, $\Delta t \neq 2\tau/(2m - 1)$ and $\Delta t \eta_\varepsilon \neq -2$, there is a period-(2, 1) solution $U^n \equiv U_*^n e$, where

$$U_*^n = \frac{(2 + \Delta t \eta_\varepsilon)}{2(m\Delta t - \tau)} \left[ 1 + (-1)^n \sqrt{\frac{\Delta t(\eta_\varepsilon[(2m - 1)\Delta t - 2\tau] - 2)}{(2 + \Delta t \eta_\varepsilon)[(2m - 1)\Delta t - 2\tau]}} \right]. \tag{4.1}$$

If $m$ is even, $\Delta t \neq 2\tau/(2m - 1)$ and $\Delta t \eta_\varepsilon \neq -2$, there is a period-(2, 1) solution with

$$U_*^n = -\frac{(2 + \Delta t \eta_\varepsilon)}{2[(m - 1)\Delta t - \tau]} \left[ 1 + (-1)^n \sqrt{\frac{\Delta t(\eta_\varepsilon[(2m - 1)\Delta t - 2\tau] + 2)}{(2 + \Delta t \eta_\varepsilon)[(2m - 1)\Delta t - 2\tau]}} \right]. \tag{4.2}$$

The solutions (4.1) and (4.2) only exist when the term in the square root is positive. Note that in both cases we are also assuming $\Delta t > \tau$ if $m = 1$ and $\tau/m < \Delta t < \tau/(m - 1)$ if $m > 1$.

## 4.2.1. Period-(2, 1) for N = 2

The regions of stability for the solutions (4.1) and (4.2), where $\eta_\varepsilon = 1 - 8\varepsilon$, can be determined numerically. Let the symbols "$*$" and "$\circ$" mark the region in which the period-(2, 1) solution is stable for $m$ odd and $m$ even, respectively.
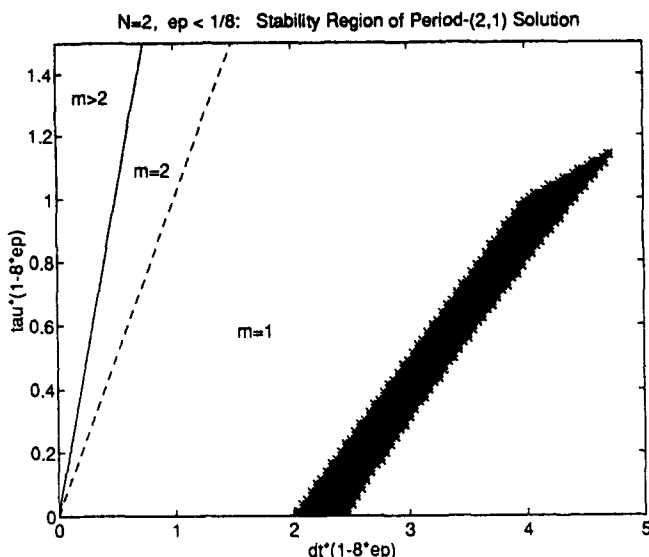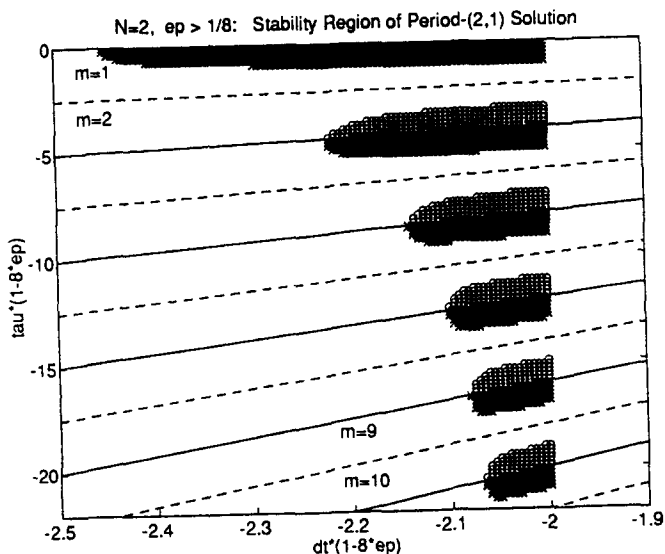
Fig. 6. Stability region for the period-(2, 1) solution when $\varepsilon < \frac{1}{8}$ in the $\Delta t(1 - 8\varepsilon) - \tau(1 - 8\varepsilon)$ plane.

When $\varepsilon < \frac{1}{8}$, the stability region is given in Fig. 6. Note that it lies within the area where $m = 1$; this solution bifurcates from the stepsize $\Delta t = 2(\tau \eta_\varepsilon + 1)/\eta_\varepsilon$ at which the nonzero solution $U^n \equiv \eta_\varepsilon e$ becomes unstable.

When $\varepsilon > \frac{1}{8}$, the stability regions for $m = 1, \ldots, 11$ are given in Fig. 7. Note that as $m$ increases the size of the region in which the solution is stable shrinks. This solution is bifurcating from the stepsize $\Delta t = -2/\eta_\varepsilon$ at which the zero solution becomes unstable.



Fig. 7. Stability region for the period-(2, 1) solution when $\varepsilon > \frac{1}{8}$ in the $\Delta t(1 - 8\varepsilon) - \tau(1 - 8\varepsilon)$ plane.
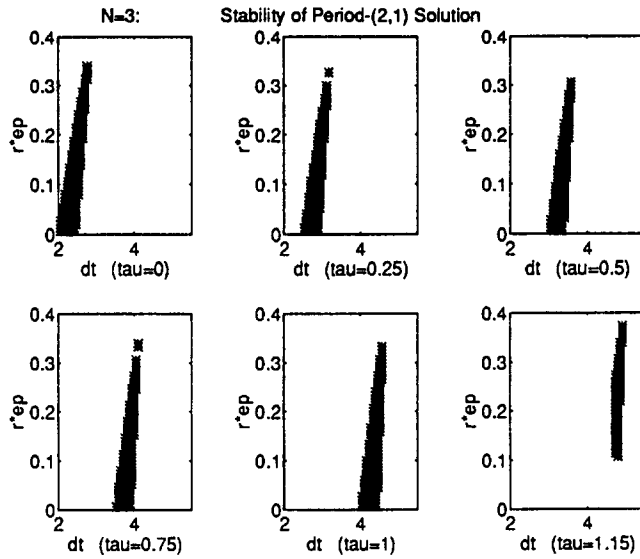
Fig. 8. Stability regions for the period-(2, 1) solution when $\Phi_1(t) \neq \Phi_2(t)$, for various $\tau$, in the $\Delta t - r_\varepsilon$ plane.

### 4.2.2. Period-(2, 1) for N = 3

Consider the case $N = 3$ for which $\eta_\varepsilon = 1 - 9\varepsilon$. When $\Phi_1(t) \neq \Phi_2(t)$, the numerically determined linear stability regions of the solutions (4.1) and (4.2), at some selected values of $\tau$, are given in Fig. 8. When $\Phi_1(t) = \Phi_2(t)$, the linear stability region is shown in Fig. 9, for $\Delta t, r_\varepsilon \in (0, 15)$, at some selected values of $\tau$. The regions are plotted in the $\Delta t - r_\varepsilon$ plane.
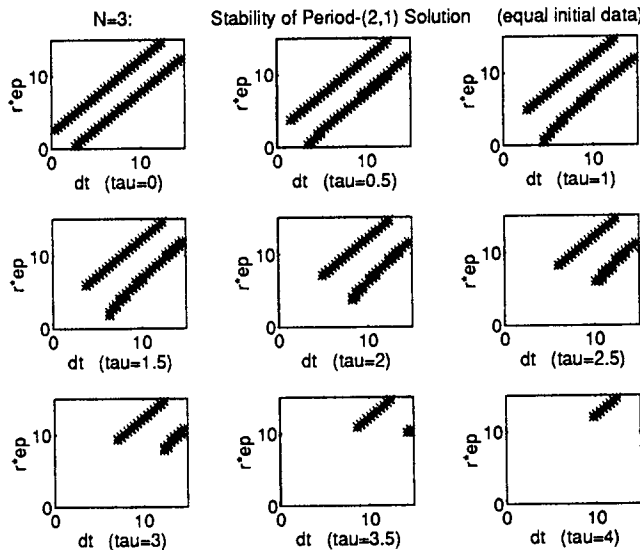


Fig. 9. Stability regions for the period-(2, 1) solution when $\Phi_1(t) = \Phi_2(t)$, for various $\tau$, in the $\Delta t - r_\varepsilon$ plane.
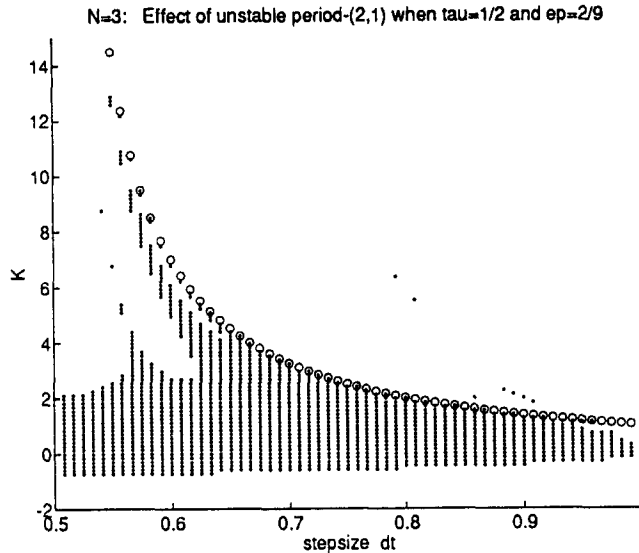
Fig. 10. Effect of the unstable period-(2, 1) solution on the stable period-(1, 1) solution, with $\Phi_1(t) = \Phi_2(t)$, in the $\Delta t - \mathcal{K}$ plane.

Unstable solutions will not be computed in practice. However, as pointed out in [16], they may have a significant impact on the dynamics. To illustrate this, consider the case $\tau = \frac{1}{2}$ and $\varepsilon = \frac{2}{9}$. With initial values $\Phi_1(t) = \Phi_2(t)$, the zero solution is stable for $0 < \Delta t < 2$. With $\frac{1}{2} < \Delta t < 1$, for which $m = 1$, the period-(2, 1) solution (4.1) exists and is unstable. In our tests the iteration is initiated with

$$v^0 = \begin{bmatrix} U^0 \\ U^{-1} \end{bmatrix} \in \mathbb{R}^4,$$

where

$$\{U^0, U^{-1}\} = \mathcal{K}\left[ 1 \pm \sqrt{\frac{\Delta t(1 + \Delta t)}{(2 - \Delta t)(1 - \Delta t)}} \right] e.$$

In Fig. 10 the value $\mathcal{K}$ is allowed to vary from $-2$ to 15 and the symbol "·" is displayed in the $\Delta t - \mathcal{K}$ plane if the iterates converge to zero. The symbol "∘" marks, for each stepsize, the value $\mathcal{K} = (2 - \Delta t)/(2\Delta t - 1)$ at which the initial data reaches the period-(2, 1) solution in (4.1). It can be seen in Fig. 10 that for a significant range of $\Delta t$ the unstable period-(2, 1) solution roughly corresponds to the boundary of the basin of attraction of the stable zero fixed point.

## 5. Summary

Our aim in this work was to study the existence and stability of the basic steady states of a discretised version of Hutchinson's equation (2.1), and to examine the bifurcations to spurious,

periodic solutions. The report [4] (which considers a range of nonlinear reaction terms) gives information about the case where $\tau = 0$. In this work we extended these results in various ways. In particular, we showed that period-$(2, 2)^*$ solutions play an important role in the bifurcation that occurs at the linear stability limit. New results were then derived for the general case of $\tau > 0$. Introducing the extra parameter $\tau$ changes the recurrence from a one-step map to an $m$-step map, where $m$ depends on the ratio of the delay to the time step. Typically, the analysis for $m > 2$ is intractable, and hence numerical computations must be used to examine the behaviour.

It has been pointed out in several references, including [4,6,7,16,18], that a rich variety of behaviour is possible when the time step exceeds the standard linear stability limit. This work serves as further illustration of this phenomenon but, more importantly, provides insights in two main areas.

*The effect of a delay*

In comparing the $\tau = 0$ and $\tau > 0$ cases, the first point to be made is that the stability of the zero fixed point is unaffected by $\tau$. (This is a consequence of the fact that the delay term in (2.1) disappears on linearising about $u \equiv 0$.) For the nonzero fixed point, Fig. 3 summarises the results for $N = 2$, and also for $N = 3$ when the initial data is symmetric. In both cases, increasing $\tau$ a small distance away from zero causes the fixed point to become stable for a larger range of time steps. As $\tau$ is increased further, the range of stable time steps shrinks, reaching zero when the semi-discrete problem itself becomes unstable. For the case where $N = 3$ and the initial data is not symmetric, Fig. 5 gives stability regions for the nonzero fixed point at various $\tau$. Once more, a small delay increases the stability range, but larger values cause the region to shrink. Overall, our results are in agreement with other examples where hereditary effects are introduced, such as those in [9], where *introducing a small delay improves stability of the true fixed point*.

We also found that for $\tau > 0$ spurious solutions may exist for *time steps that are stable in the linear sense*. As illustrated in Fig. 10, even *unstable* spurious solutions can be important, since they generally influence the basin of attraction of the "correct" solution.

*Symmetry*

In the $N = 3$ case, our analysis was refined to account for the symmetry in the problem. We showed that, even allowing for finite precision arithmetic, there is a dramatic difference in the bifurcation patterns that arise with equal and unequal initial data; see Fig. 2.

We conclude by mentioning two possible extensions to this work. First, in the case where $\tau = 0$, the fully continuous problem (2.1) has been widely studied, and it is known that for $\varepsilon < 1/\pi^2$ a stable, positive, time-independent steady state exists, having the form $u(x, t) = v(x)$, where $v(x)$ solves the second-order ODE $\varepsilon v''(x) + v(x)(1 - v(x)) = 0$, with $v(0) = v(1) = 0$. Details can be found, for example, in [12]. It would be of interest to study the existence and stability of an analogous steady state for the discrete problem, both for $\tau = 0$ and $\tau > 0$. A major difficulty here seems to be the characterisation of the spatial pattern of the solution for general $N > 2$. A second area of study is the use of variable time steps. Although constant grid spacing is commonly used, particularly in the solution of PDEs, there is practical and

theoretical evidence to show that variable time-stepping via error control is helpful for long-time simulation, particularly as a means of avoiding spurious behaviour; see [1]. Some analysis of an error-control scheme for the DDE version of (2.1), that is, with $\varepsilon = 0$, has been given in [9]. It would be of interest to see how these ideas, which are based on the work of [8,10], could be extended to the PDE case with delay.

# References

[1] M.A. Aves, D.F. Griffiths and D.J. Higham, Does error control suppress spuriosity?, Tech. Report NA/155, University of Dundee (1994); also: *SIAM J. Numer. Anal.* (to appear).

[2] R. Bellman and K.L. Cooke, *Differential-Difference Equations* (Academic Press, New York, 1963).

[3] G. Friesecke, A global bifurcation result for a delay-diffusion equation, Tech. Report No. 92, University of Bonn.

[4] A.R. Gardiner and A.R. Mitchell, Bifurcation studies in long time solutions of discrete models in reaction diffusion, Tech. Report NA/136, University of Dundee (1992).

[5] P. Glendinning, Island chain models and gradient systems, *J. Math. Biol.* 32 (1994) 171–178.

[6] D.F. Griffiths and A.R. Mitchell, Stable periodic bifurcations of an explicit discretization of a nonlinear partial differential equation in reaction diffusion, *IMA J. Numer. Anal.* 8 (1988) 435–454.

[7] D.F. Griffiths, P.K. Sweby and H.C. Yee, On spurious asymptotic numerical solutions of explicit Runge–Kutta methods, *IMA J. Numer. Anal.* 12 (1992) 319–338.

[8] G. Hall, Equilibrium states of Runge–Kutta schemes, *ACM Trans. Math. Software* 11 (1985) 289–301.

[9] D.J. Higham, The dynamics of a discretised nonlinear delay differential equation, in: D.F. Griffiths and G.A. Watson, eds., *Numerical Analysis 1993* (Longman Scientific and Technical, 1994) 167–179.

[10] D.J. Higham and I.T. Famelis, Equilibrium states of adaptive algorithms for delay differential equations, *J. Comput. Appl. Math.* (to appear).

[11] D.J. Higham and T. Sardar, Existence and stability of fixed points for a discretised nonlinear reaction-diffusion equation with delay, Tech. Report NA/156, University of Dundee (1994).

[12] D.S. Jones and B.D. Sleeman, *Differential Equations and Mathematical Biology* (George Allen and Unwin, 1983).

[13] J.P. Keener, Propagation and its failure in the discrete Nagumo equation, in: B.D. Sleeman and R.J. Jarvis, eds., *Ordinary and Partial Differential Equations* (Longman Scientific and Technical, 1987) 95–112.

[14] A.R. Mitchell and D.F. Griffiths, *The Finite Difference Method in Partial Differential Equations* (Wiley, New York, 1985).

[15] J.D. Murray, *Mathematical Biology* (Springer-Verlag, Berlin, 2nd ed., 1993).

[16] A.M. Stuart and A.T. Peplow, The dynamics of the theta method, *SIAM J. Sci. Statist. Comput.* 12 (1991) 1351–1372.

[17] J.M.T. Thompson and H.B. Stewart, *Nonlinear Dynamics and Chaos* (Wiley, New York, 1986).

[18] H.C. Yee, P.K. Sweby and D.F. Griffiths, Dynamical systems approach study of spurious steady state numerical solutions of nonlinear differential equations. 1. The ODE connection and its implications for algorithm developments in computational fluid dynamics, *J. Comput. Phys.* 97 (1991) 249–310.